Research Article GU J Sci 36(4): 1538-1551 (2023) DOI: 10.35378/gujs.1146050

Gazi University

Journal of Science

http://dergipark.gov.tr/gujs

Magnetic Separation of Micro Beads and Cells on a Paper-Based Lateral Flow System

Muhammed Fuad FAROOQI, Kutay ICOZ *

Electrical and Electronics Engineering Department, Abdullah Gül University, 38030, Kayseri, Türkiye

Highlights

- This paper focuses on paper based magnetophoretic system develop for cell separation.
- Cells observed with a low-cost setting, no fluorescent labeling.
- Simple but time-efficient image processing method developed to analyze paper samples.
- At worst case scenario, minimum 90% cells traveled on the paper-based lateral flow system.

Article Info

Received: 20 July 2022
Accepted: 06 Oct 2022

Keywords

Paper based lateral assay,
Image processing,
Magnetophoresis,
Cancer cells,
Bright-field optical microscope

Abstract

Paper based lateral flow systems are widely used biosensor platforms to detect biomolecules in a liquid sample. Proteins, bacteria, oligonucleotides, and nanoparticles were investigated in the literature. In this work we designed a magnetic platform including dual magnets and tested the flow of micron size immunomagnetic particles alone and when loaded with cells on two different types of papers. The prewetting conditions of the paper and the applied external magnetic field are the two dominant factors affecting the particle and cell transport in paper. The images recorded with a cell phone, or with a bright field optical microscope were analyzed to measure the flow of particles and cells. The effect of prewetting conditions and magnetic force were measured, and it was shown that in the worst case, minimum 90% of the introduced cells reached to the edge of the paper. The paper based magnetophoretic lateral flow systems can be used for cell assays.

1. INTRODUCTION

In recent years, considerable efforts have been made to develop biosensors made of cellulose-based materials due to significant advantages such as being low-cost, disposable, portable and having fast response time [1]. Lateral flow biosensors (LFBs) are paper based devices where analyte flow across the porous medium and tested for specific interactions with the receptors immobilized on the surface. Various types of nanoparticles such as gold, fluorescent, polystyrene, magnetic and carbon were incorporated with LFBs as colorimetric labels [2]. Even though LFBs can have high sensitivity, low limit of detection and good selectivity, LFBs have their own drawbacks as well, usually the response obtained from them is through the naked eye which would give qualitative results and not quantitative results. This problem can be solved by taking the images of the LFBs and then using image analysis methods to quantify the output signal [3, 4]. The other drawback is that the sample needs to be in a fluidic state to be run through the paper [5]. LFBs are not limited to detect biomolecules but also used to detect hazardous materials, heavy metals, allergens and pathogens in food, pesticides and drugs [6–12]. Even though there are many articles reporting detection of small biomolecules such as proteins, nucleic acids, exosomes, and enzymes [2, 13], there are not much research has been done with cells. The small pores in the LFBs are not ideal for the movement of large cells, however LFBs have great potential and reported for cell detection [14]. In one study, LFB was developed to detect human pluripotent stem cells by forming a sandwich assay on a nitrocellulose membrane. The accumulation of antibody conjugated gold nanoparticles on the membrane created visual signals which resulted in detection of 10,000 stem cells [15]. In another study, CD45+ cells were tagged

*Corresponding author, e-mail: kutay.icoz@agu.edu.tr

with antibody conjugated gold nanoparticles and trapped in the paper, colorimetric intensity measurements of gold nanoparticles resulted in counting 60,000- 160,000 cells [14].

Magnetic particles and external magnetic fields were also incorporated with LFBs for separation and preconcentration of target proteins [16]. Besides the isolation of target biomolecules [17], magnetic particles have also other advantages which make them attractive for biosensors such as signal amplification [18,19], sensitivity enhancement [20] and visual labeling [21, 22].

In this study, an LFB incorporating micron size immunomagnetic beads and external magnetic field is designed and the impact of two main parameters (external magnetic field and prewetting of the paper) on cell movement were investigated. There are not many applications of paper-based systems for cell detection in the literature, the aim of this study is to explore the parameters of a magnetophoretic paper-based system so that further immunomagnetic separation and LFB can be combined, and paper-based systems can be used for cell detection and analysis.

1.1. Magnetic Force

The force balance on a moving magnetic particle in a microfluidic system is expressed in Equation (1)

$$m_p \frac{du_p}{dt} = F_m + F_g + F_d + F_B + F_L \quad (1)$$

where the mass of the particle is m_p, the particle velocity is u_p. F_m, F_g, F_d, F_b and F_L are magnetic force, gravity force, drag force, Brownian force and lift force respectively and the magnetic force is dominant for micron size particles [23]. The magnetic force on a magnetic particle is

$$F_m = \frac{V_p \Delta\chi}{2\mu_0} (\boldsymbol{B}.\nabla)\boldsymbol{B} \quad (2)$$

where V_p is the volume of the particle, $\Delta\chi$ is the difference between magnetic susceptibilities, B magnetic field, μ_0 is the magnetic permeability [24]. In [25], it was reported that the electromagnets generated 50-100 mT magnetic field and induced approximately 25 pN magnetic force on a micron size magnetic particle.

1.2. Fluid Flow in Paper

Fluid flow in paper due to the capillary action was modeled using different approaches. The Lucas-Washburn Equation -the classical model- is used to explain the fluid in a porous media and assumes that the porous media is composed of parallel bundle of capillary tubes that have the same diameter (Equation (3)) [26]. The distance travelled by the fluid front due to capillary pressure (L) is a function of wicking time (t), fluid and material properties:

$$L^2 = \frac{\gamma \cos(\theta) r}{2\mu} t \rightarrow L^2 = kt \,, \quad (3)$$

r is the effective pore radius, γ is the surface tension, θ is the liquid- contact angle and μ is the fluid viscosity, k is the slope of L^2 -t graph can be named as diffusivity [27]. To have more accurate fluid flow predictions, alternative models were also developed, such as Darcy's law [28]. One alternative model is based on heterogenous pores composed of various tube diameters and provided improved predictions for transportation over long distances [29].

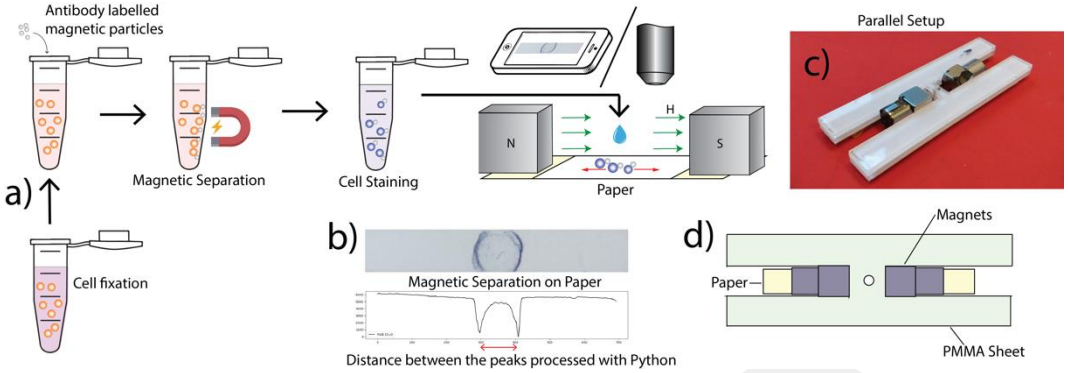

Figure 1*. a) Illustration of the paper based magnetophoresis of cells and magnetic particles, b) Image of the paper and output of the image processing c) Image of the magnetic platform d) Illustration of magnetic platform and the paper*

Schematic illustration of the magnetophoretic LFB for cell and micron size magnetic particle movement is in shown in Figure 1. Target cells are first fixed and then captured by antibody conjugated immunomagnetic beads. To visualize cells on paper, cells were stained with Trypan blue. The stained cells were introduced to the mid-point of the paper where a parallel magnetic field was applied with magnets having opposite magnetic poles. Either a cell phone or a bright field optical microscope is used to record the images of the magnetic particles and the cells. The images were analyzed using an algorithm developed in Phyton. This study reports the impact of the magnetic field and prewetting on the separation distance and accumulation intensity of magnetic particles and cells.

2. MATERIAL METHOD

2.1. Magnetic Platform and Simulation

The magnetic platform was created using 4 Neodymium magnets (grade N52) as shown in Figure 1. Two cube shaped magnets of dimensions 1.2 cm x 1.2 cm x 1.2 cm and two cylindrical magnets of dimensions 1.2 cm x 1.2 cm. The concept was creating a concentrated magnetic field between the two magnet sets. The magnets were held together using 2 H shaped pieces of 3.175 mm thick acrylic sheets. The magnets were placed into the acrylic sheet sandwich. The H-shaped platform allowed to change the distance between the magnets, thus the applied magnetic field was altered.

The finite element model of the magnetic platform was built using the modeling software COMSOL Multiphysics® 5.2. The magnetic field between the two magnets were calculated in COMSOL.

2.2. Cell Preparation

The myelogenous leukemia cell line K562, were obtained from American Type Culture Collection (ATCC), was cultured in RPMI medium. First the cells were centrifuged for 4 minutes and washed. Then the cells were counted under microscope and fixed with paraformaldehyde. For 3 million cells, 3 ml of paraformaldehyde and 3 ml of PBS was used. Later, the cells were placed onto a MACS rotator for 15 minutes followed by centrifuge and washing with PBS three times. MACS buffer was prepared using, 10 mg of BSA, 20 µl of EDTA in 10 ml of PBS. Invitrogen Dynabeads CD45 (Thermo Fisher Scientific, Waltham, Massachusetts) were washed using MACS buffer. 20 µl of Dynabeads were added to 1 ml of the cell solution in MACS buffer. The sample was then put onto the rotator at 4°C for 15 minutes. The cells were washed using PBS and a magnetic rack. To stain the cells, 0.5% trypan blue solution was used. 500 µl of cell solution was mixed with 500 µl of trypan blue solution. The solution was left for 5 minutes after which it was washed 3 times with PBS using the magnetic rack. Then a 300 µl solution was created with PBS.

2.3. Paper Preparation

Two kinds of paper were used Millipore Hi-Flow™ Plus 75(HF075) and Hi-Flow™ Plus 135(HF135). HF075 has larger pore size has higher flow rate compared to HF135. A design was created for cutting the paper in CorelDRAW (Corel Corporation, Ottawa, Ontario, Canada). The paper was cut into strips of size 5 cm x 0.5 cm by using Epilog Model 10000 30 Watts laser cutter (Epilog Laser, Golden, Colorado, USA).

2.4. Magnetic Force Experiments

Dynabead superparamagnetic beads of 4.5 μm diameter, conjugated with CD45 antibody were used for the experiments. The magnetic field was varied by changing the distance between the magnets. The distance was varied from 2.5 cm (87.7 mT) to 8.0 cm (8.3 mT) and the magnetic field was measured with a gaussmeter (Sypris/FW Bell, Orlando, FL, USA). The HF075 paper was first wetted using 30 μl deionized water and then the sample was introduced. The magnetic field was applied for 10 minutes after which images were acquired using either a cellphone or bright-field optical microscope and processed using the Python code.

2.5. Cell Experiments

The papers were first wetted using 30 μl 1% BSA in PBS solution. Under various magnetic fields, the travel time of cells from middle point to the edge of the paper was measured when a visible accumulation is observed at the edge of the paper. Images of the samples were recorded and then processed.

2.6. Cell Viability and Prewetting

The cell viability was measured under various prewetting conditions; no wetting, PBS, and BSA/PBS. After wetting the paper, the paper was left for 10 minutes to wick the liquid and then the sample was introduced on the paper, and a video was recorded using the microscope system. The time taken for the cells to burst and lose color was observed and recorded.

2.7. Image Processing

The optical micrographs were recorded either using the optical microscopy system connected to a CCD camera (Nikon Instruments, Melville, NY, USA) or a cell phone (ONEPLUS 5T, Oneplus, Shenzen, China). The images of the sample were processed using a code written in Python 3. The code would take the cropped images which would just include the test are of the paper. The pixel values of the images were used to create a graph. Each of the Y-axis values were added at each of the points of the X-axis and then a 2D graph was plotted. Brighter areas on the paper resulted in a higher value on the graph whereas darker areas resulted in lower values on the graph. The code would also detect 2 of the peaks that would be formed on the paper by the accumulation of the sample. The code calculated the distance between the two accumulation sites and plot them on the graph. The amplitudes of the peaks were also measured from the graphs to find the accumulation levels.

2.8. Statistical Analysis

Cell and paper comparison experiment was repeated at least three times to obtain the means and standard deviations of the data; the error bars indicate the standard deviation from the average values. Independent samples student t-test was performed for the experimental results. Statistical significance was considered at $P < 0.05$.

3. THE RESEARCH FINDINGS AND DISCUSSION

3.1. Magnetic Platform

First the change in the magnetic field with respect to distance of a single magnet was investigated and as expected, there was an exponential decrease in the magnetic field (Figure 2a). The two-magnet setup was simulated in COMSOL (COMSOL, Inc., Burlinghton, MA, USA) (Figure 2b). Then the magnetic field between the two magnets was measured by placing the probe of the gauss meter between the magnets, when the magnets were set to 2.75 cm apart from each other (Figure 2c). The simulation results also produced a similar trend in the change of magnetic field with respect to the position between the magnets (Figure 2d). In order to obtain a uniform magnetic field in the middle of the paper and increase the magnetic field two magnet setup was preferred. However, it is not necessary to use two magnets, using one magnet is also possible as long as the sufficient magnetic field is generated. As seen from the Figure 2, when compared to the middle point the magnetic field exponentially increased towards the surface of magnets.

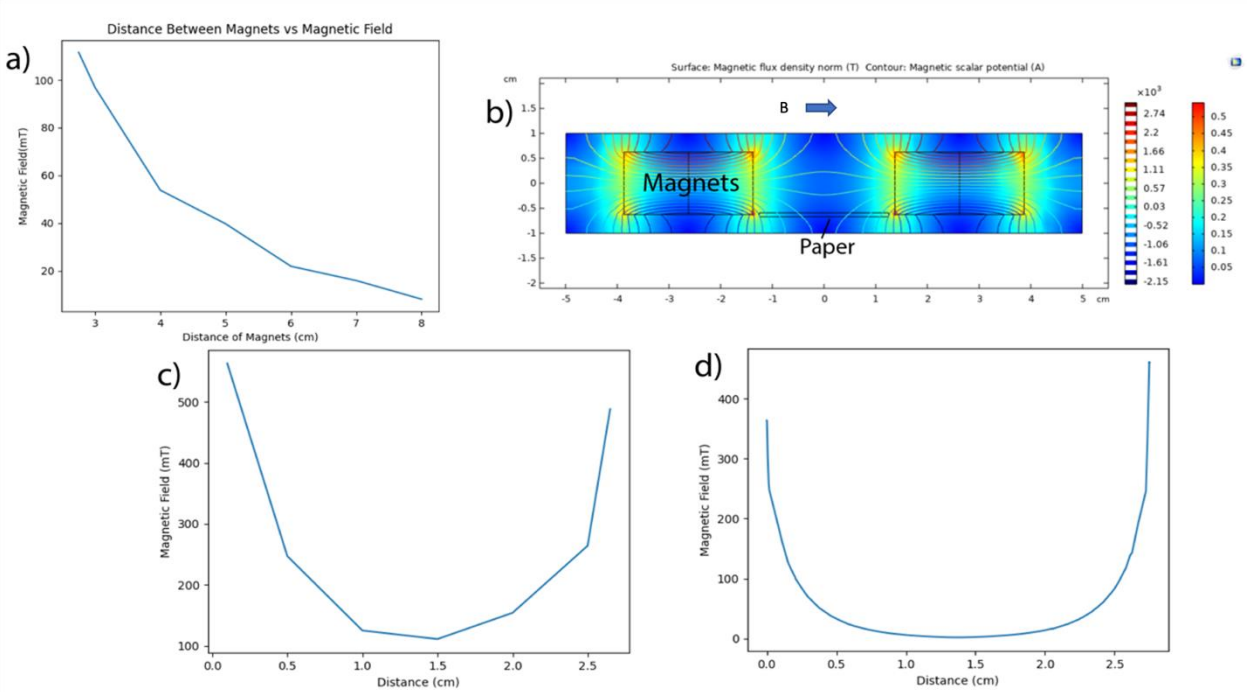

Figure 2. *a) Variation of the magnetic field with respect to distance from one magnet, experimental measurement. b) COMSOL simulation of the magnetic platform c) Variation of the magnetic field as the position of the probe is changed between the magnets, experimental measurement. d) Simulation of the setup in b*

3.2. Magnetic Field Effect on Immunomagnetic Particle Movement

The micron size immunomagnetic particles (without cells) were introduced to the middle of the HF075 paper after 30 µl of wetting. As seen in Figure 3, the applied external magnetic field was altered (first column), and the movement of the particles were analyzed. From the pixel distribution graphs, the distance between the peaks and the amplitude of the peaks with respect to base line were measured. The distance travelled and the peak amplitudes were plotted in Figure 3b. As the magnetic field increased the amplitude also increased which means that the accumulations of the particles were intense. In the case of weak magnetic fields (<30 mT), magnetic beads did not completely accumulate at the edge of the paper. In order to transport most of the beads towards the edges of the paper, a magnetic field of 88 mT was required. We observed that for the micron size particles, magnetic force is dominant among other forces as presented in Equation (1).

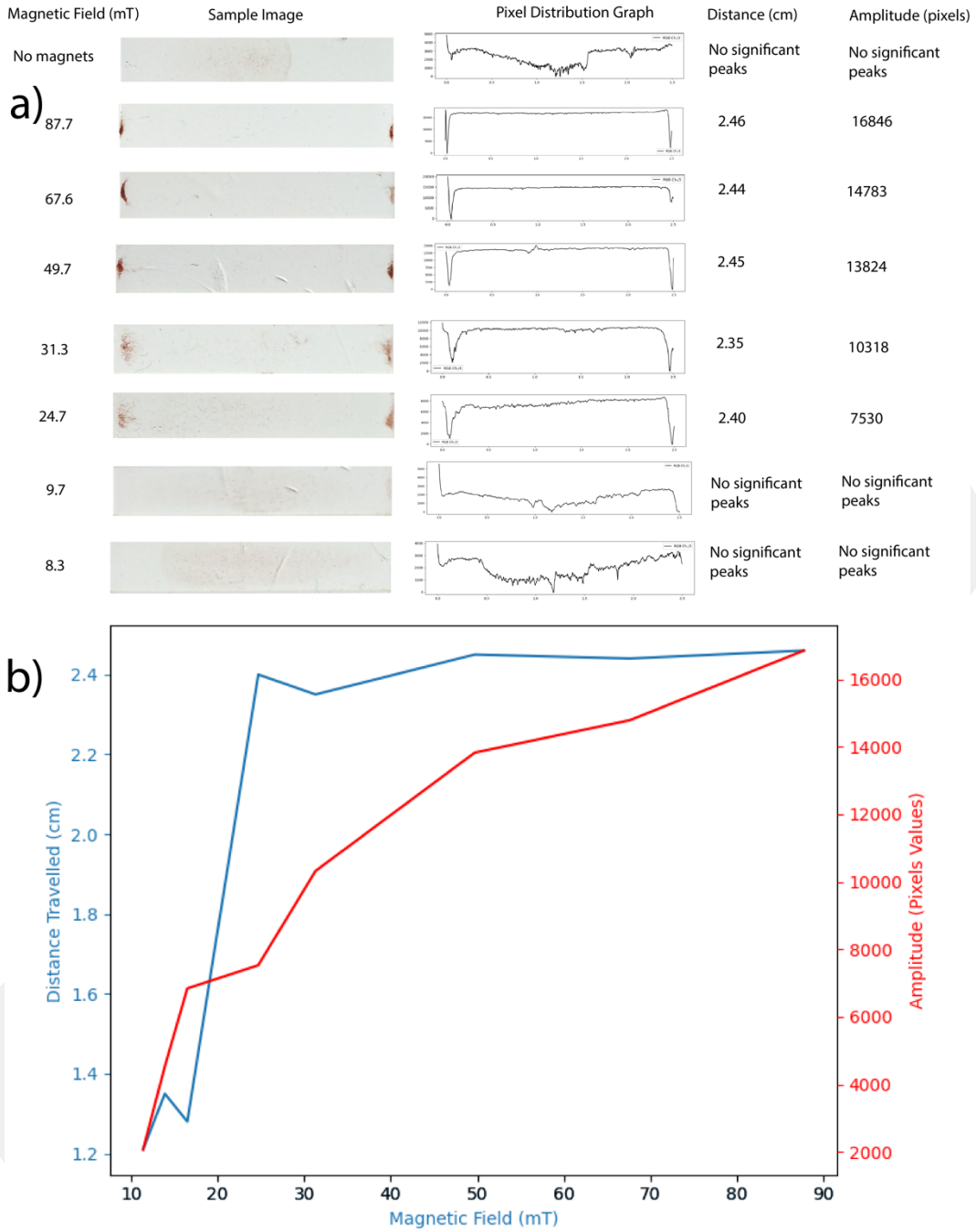

Figure 3*. a) Cell phone images of the papers for various magnetic fields and the output graphs of the image processing algorithm showing the distance traveled by the particles and the amplitude of the peaks. b) Graph of magnetic field vs distance moved in blue and the amplitude of the peaks graph in red*

3.3. Prewetting Effect on Immunomagnetic Particle Movement

To reveal the impact of prewetting on the movement of immunomagnetic particles, various prewetting conditions were tested using HF135 paper. As the wetting was increased the particles move longer distances and accumulate more (Figure 4). 10 µl and 15 µl of wetting were not sufficient to move magnetic particles towards the edge of the paper. A magnetic field of 244.7 mT was applied and to achieve this magnetic field, a distance of 1.5 cm was set up between the magnets. After 20 µl of wetting, the magnetic beads started moving towards to the magnets, so the distance between the magnets was changed to 2.75 cm which resulted in a magnetic field of 113.3 mT. The graph in Figure 4 includes both conditions. Even though the

magnetic field decreased, the wetting of the paper is dominant and magnetic particles accumulate towards the edges.

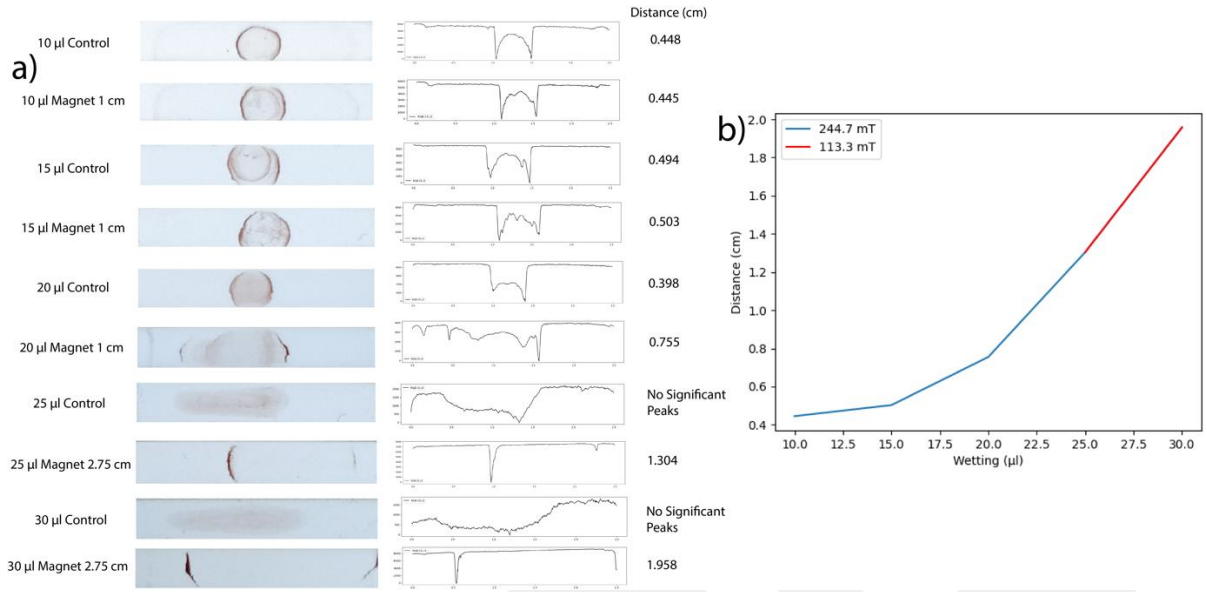

Figure 4. *a) Cell phone images of the samples and the results of image processing code. b) The graph shows the distance travelled with respect to prewetting conditions*

3.4. Comparison of HF075 and HF135 Papers

According to the manufacturer HF075 has a mean pore size of 14.5 ± 4.7 µm whereas HF135 has a mean pore size of 11.6 ± 4.06 µm. The two papers were compared in detail in terms of fluid flow and found that HF075 has higher diffusivity compared to HF135 [27]. In our experiments, the effect of the papers on magnetic particle travel distance was also investigated. 30 µl of wetting was applied along with a magnetic field of 110.2 mT. It was found that HF075 paper allowed particles to travel longer distance and to separate more, (Figure 5). The results agree with the higher diffusivity of HF075 compared to HF135 in Equation (2).

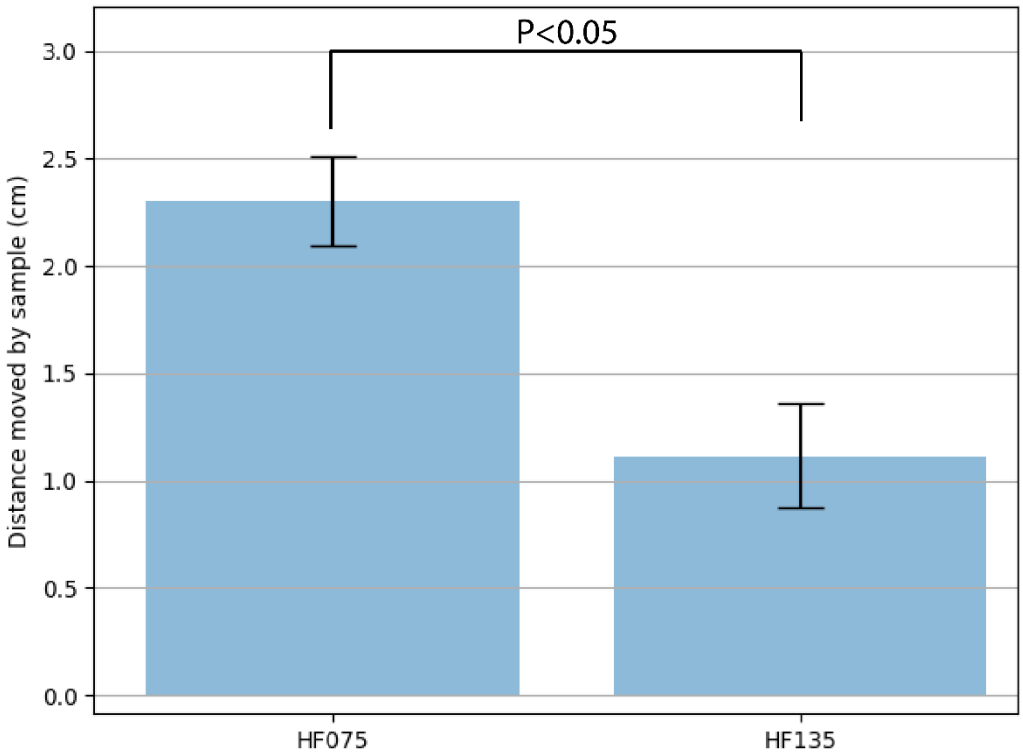

Figure 5. *Distance moved by magnetic particles on the two papers at 30 µl wetting*

3.5. Prewetting and Cell Viability

In the previous section we compared the two papers, in this section we focused on the cell viability for the less diffusive paper. Although the paper is not an ideal environment for the large cells, paper-based systems have great potential for pump-free fluidic flow and low-cost biosensors [14]. The prewetting of the paper (HF135) not only improved the separation of the cells, but it also assisted in the viability of the cells. As the paper dried up, the cells shrank and then broke apart. This could be because of osmosis as the water diffused out of the cell. Under no wetting conditions the cells quickly lost their membrane structure but when PBS was added to the prewetting solution, it took longer time for cells to lose their membrane structure and with BSA/PBS prewetting, cell viability was improved as seen in Figure 6.

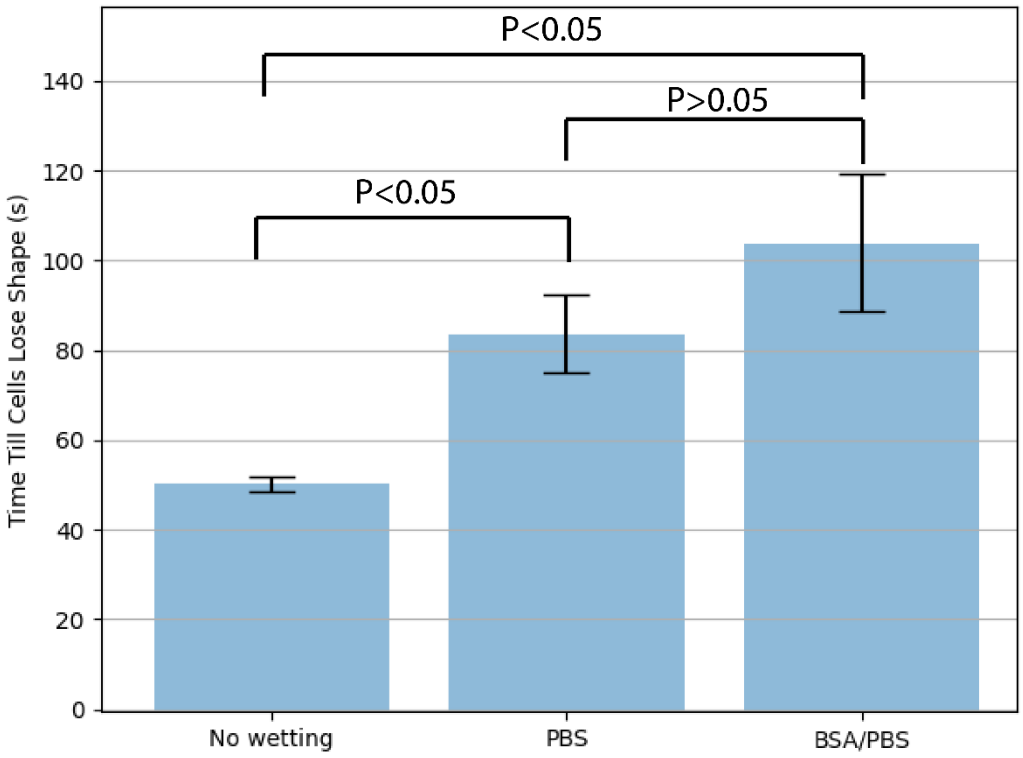

Figure 6. *The impact of prewetting of paper on cell viability*

3.6. Cell Experiments

The papers were wetted with 30 µl of BSA/PBS solution and under the various external magnetic field, the travel time of immunomagnetic beads loaded with cells on the paper was measured (Figure 7). Also, for both paper types, stained cells were captured with immunomagnetic particles and traveled under the applied external magnetic field. 2700 cells were introduced to the paper prewetted with BSA/PBS and 90% of the cells reached to the edge of the papers (Figure 8).

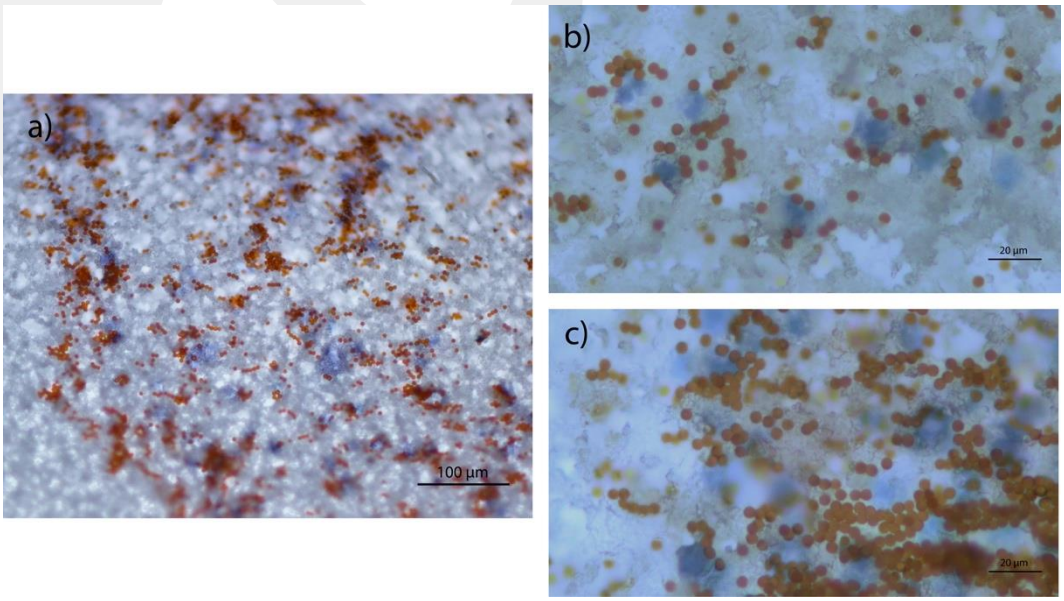

Figure 7. *a) Bright filed optical microscope images of cells (stained with blue) at the edge of the paper b) Cells in the middle of the paper (no magnet condition) c) cells at the edge of the paper (magnetic condition)*

As the magnetic field increased, the required time for the cells to reach to the edge of the paper decreased. When the magnetic field is less than 16 mT, then there was no significant accumulation at the edge. At 111.6 mT it took the least time for the cells to reach the edges. There was an exponential decrease in time for the cells to reach the edges of the paper with respect to magnetic field.

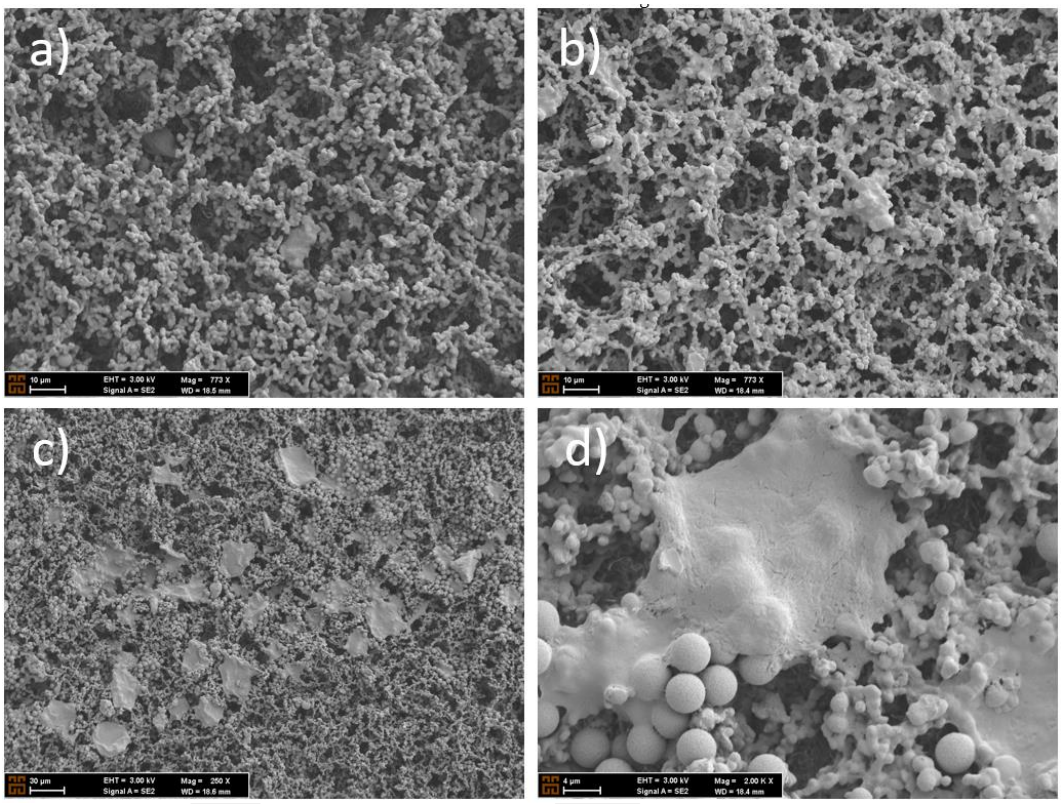

Figure 8. *a) HF075 paper SEM image b) HF135 paper SEM image c) Magnetic beads and cells on HF075 paper d) Magnetic beads and cells on HF135 paper*

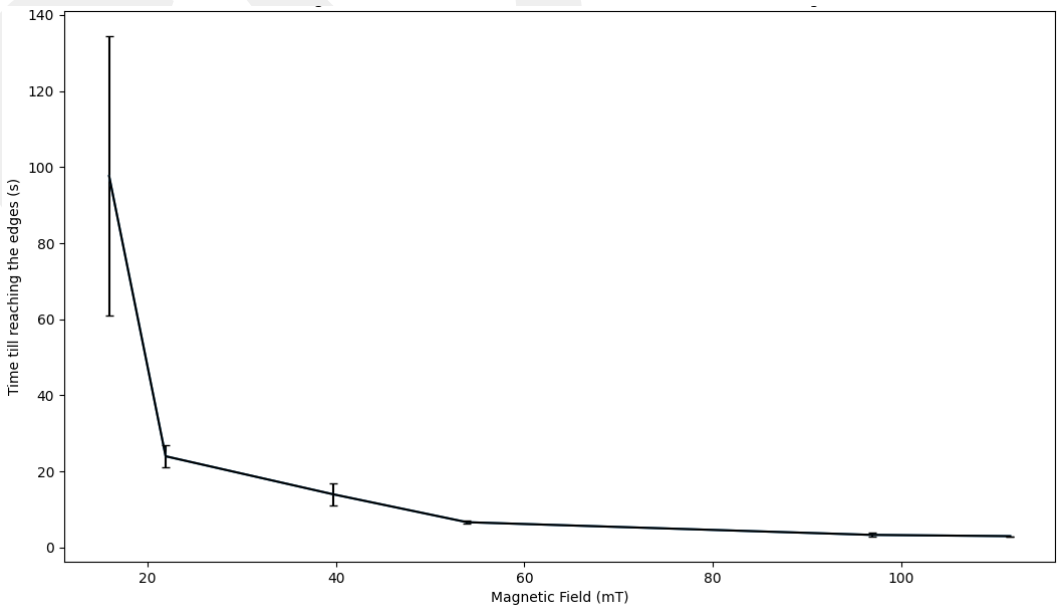

Figure 9*. Travel time for the cells to reach the edges with respect to the magnetic field.*

By using Figure 9 and Equation (3), the k (diffusivity, Equation (3)) values were calculated as 1.6, 6.5,11.2, 23.4, 46.9, and 52.1 for the increasing magnetic fields in the range of 16 mT to 111.6 mT. These data indicates that the higher magnetic field results in higher fluid diffusivity in the paper membrane.

4. RESULTS

The porous nitrocellulose membranes are not the ideal platforms for large cells, however due to the great potential of paper-based systems, special design efforts are needed [14]. In this work to overcome the limitations of LFBs for cell assays, we proposed to apply external magnetic field and incorporate magnetic particles. The effects of magnetic field and wetting were investigated to reveal the flow of micron size particles and cells on the paper. By applying sufficient magnetic fields and wetting, cells and magnetic particles were traveled approximately 1.25 cm on the paper. It was observed that the sufficient magnetic field was able to accumulate the particles at the edge of the paper if the paper was appropriately wetted. The permanent magnets induced approximately 100 pN force on each magnetic particle in the middle of the paper. The developed image processing algorithm was able to measure the accumulation amount and travel distance. Measuring the amplitude of the peaks also allowed the understanding of the distribution of the magnetic particles and cells on the sample paper. At higher magnetic fields there were accumulations of the particles at the edge of the paper and less distribution of the cells in the center regions of the paper. Wetting is a strong parameter affecting the separation of the particles. It was noted that as the wetting was increased, the particles travelled longer distances. This was because wetting would allow the sample to move on the surface of the liquid paper interface. If the wetting was low the micron size particles were not able to move as freely. Wetting liquid also affected how long the cells survived on the paper before they were bursting due to the osmotic imbalance. The comparison of wetting conditions revealed that the cells survived longer when prewetting was performed as compared to non-wetting condition. Furthermore, cells survived significantly longer when a cell friendly buffer BSA/PBS solution was used for wetting. The cells were not able to maintain their shape for hours on paper even though they were fixed. This is probably because of the nature of the paper which is not an ideal environment for the cells and caused plasmolysis. The wetting of the paper improved the preserving the cell structure but as soon as the paper dried, the cells broke open. The environmental conditions are also important for example the wicking time of the paper is affected by the ambient temperature and humidity [30].

According to the manufacturer, the difference between the HF075 paper and HF135 paper was the flowrates and the pore sizes. The flow rate of HF135 is slower compared to HF075. In our experiments we also observed that the flow rate of HF075 is faster and liquid absorption of HF075 is slower compared to HF135 due to the density.

Magnetic field and prewetting seemed be the two most important variables in this research. Magnetic field would govern the amount of force that was applied on the sample while the wetting would govern how freely the sample was able to move. In the experiment with cells where the magnetic field was changed it was observed that as the magnetic field was increased the cells would reach the edges quicker. There was an exponential decrease in the time taken for the sample to reach the edges. The cells were moving in the liquid/ paper interface and if the paper is dry the cells and the particles are too big to go through the porous structure of the paper.

To model fluid transport in paper, Darcy's law also has been used and electrical circuit analogy can be built. Where pressure difference is equivalent to a voltage source and volumetric flow rare is equivalent to the current [28]. Our experiments showed that the external magnetic field can be modeled as an added second voltage source in series to existing voltage source into the modelling circuitry which is increasing the flow rate of the magnetic particles and the cells captured with magnetic particles.

In the worst case, minimum 90% of the cells reached to the edge of the paper where some clusters of cells and magnetic particles were got stacked in the middle. This problem can be solved by incorporating nano size magnetic particles. Paper-based systems have great advantages, they do not require complex microfabrication processes [31] and do not require external pumps as other biosensor need [32]. However, there are few research efforts on paper-based cell biosensors, and we were able to show that paper-based

magnetophoresis is a possible alternative for cell studies. Further research could be done by applying the findings of this research and using them to separate target cells from a mixed sample of cells. Then the separated cells can be introduced to a magnetophoretic paper-based device including immobilized antibody to form a sandwich assay as a low-cost, rapid point of care method.

CONFLICTS OF INTEREST

No conflict of interest was declared by the authors.

REFERENCES

[1] Dincer, C., Bruch, R., Costa-Rama, E., Fernández-Abedul, M. T., Merkoçi, A., Manz, A., Güder, F, "Disposable Sensors in Diagnostics, Food, and Environmental Monitoring", Advanced Materials, 31(30): 1806739, (2019).

[2] Quesada-González, D. and Merkoçi, A., "Nanoparticle-based lateral flow biosensors", Biosensors and Bioelectronics, 73: 47-63, (2015).

[3] Zhang, T., Wang, H. B., Zhong, Z. T., Li, C. Q., Chen, W., Liu, B., & Zhao, Y. Di., "A smartphone-based rapid quantitative detection platform for lateral flow strip of human chorionic gonadotropin with optimized image algorithm", Microchemical Journal, 157: 105038, (2020).

[4] Rey, E., Jain, A., Abdullah, S., Choudhury, T., and Erickson, D., "Personalized stress monitoring: a smartphone-enabled system for quantification of salivary cortisol", Personal and Ubiquitous Computing, 22: 867-877, (2018).

[5] Quesada-González, D. and Merkoçi, A., "Nanoparticle-based lateral flow biosensors", Biosensors and Bioelectronics, 73: 47-63, (2015).

[6] Shyu, R. H., Shyu, H. F., Liu, H. W. and Tang, S. S., "Colloidal gold-based immunochromatographic assay for detection of ricin", Toxicon, 40(3): 255–258, (2002).

[7] Mazumdar, D., Liu, J., Lu, G., Zhou, J. and Lu, Y., "Easy-to-use dipstick tests for detection of lead in paints using non-cross-linked gold nanoparticle-DNAzyme conjugates", Chemical Communications, 46(9): 1416–1418, (2010).

[8] Torabi, S. F. and Lu, Y., "Small-molecule diagnostics based on functional DNA nanotechnology: A dipstick test for mercury", Faraday Discussions, 149: 125–135, (2011).

[9] Wang, X., Li, K., Shi, D., Xiong, N., Jin, X., Yi, J. and Bi, D., "Development of an immunochromatographic lateral-flow test strip for rapid detection of sulfonamides in eggs and chicken muscles", Journal of Agricultural Food Chemistry, 55(6): 2072–2078, (2007).

[10] Leem, H., Shukla, S., Song, X., Heu, S. and Kim, M., "An Efficient Liposome-Based Immunochromatographic Strip Assay for the Sensitive Detection of SalmonellaTyphimurium in Pure Culture", Journal of Food Safety, 34(3): 239–248, (2014).

[11] Zhou, P., Lu, Y., Zhu, J., Hong, J., Li, B., Zhou, J., Montoya, A., "Nanocolloidal gold-based immunoassay for the detection of the N-methylcarbamate pesticide carbofuran", Journal of Agricultural Food Chemistry, 52(14): 4355–4359, (2004).

[12] Inoue, K., Ferrante, P., Hirano, Y., Yasukawa, T., Shiku, H. and Matsue, T., "A competitive immunochromatographic assay for testosterone based on electrochemical detection", Talanta, 73(5): 886–892, (2007).

[13] Parolo, C., Sena-Torralba, A., Bergua, J. F., Calucho, E., Fuentes-Chust, C., Hu, L., Merkoçi, A., "Tutorial: design and fabrication of nanoparticle-based lateral-flow immunoassays", Nature Protocols, 15: 3788-3816, (2020).

[14] Zhang, Y., Bai, J., Wu, H. and Ying, J. Y., "Trapping cells in paper for white blood cell count", Biosensors and Bioelectronics, 69: 121-127, (2015).

[15] Wu, W., Yu, L., Fang, Z., Lie, P. and Zeng, L., "A lateral flow biosensor for the detection of human pluripotent stem cells", Analytical Biochememistry, 436(2): 160-164, (2013).

[16] Sharma, A., Tok, A. I. Y., Lee, C., Ganapathy, R., Alagappan, P. and Liedberg, B., "Magnetic field assisted preconcentration of biomolecules for lateral flow assaying", Sensors Actuators, B Chemical, 285: 431-437, (2019).

[17] İçöz, K., Gerçek, T., Murat, A., Özcan, S. and Ünal, E., "Capturing B type acute lymphoblastic leukemia cells using two types of antibodies", Biotechnology Progress, 35(1): e2737, (2019).

[18] İçöz, K. and Mzava, O., "Detection of Proteins Using Nano Magnetic Particle Accumulation-Based Signal Amplification", Applied Sciences, 6(12): 394, (2016).

[19] Mzava, O., Tas, Z. and İçöz, K., "Magnetic micro/nanoparticle flocculation-based signal amplification for biosensing", International Journal of Nanomedicine, 11: 2619–2631, (2016).

[20] Icoz, K., Iverson, B. D. and Savran, C., "Noise analysis and sensitivity enhancement in immunomagnetic nanomechanical biosensors", Applied Physics Letters, 93(10): 103902, (2008).

[21] İçöz, K., Akar, Ü. and Ünal, E., "Microfluidic Chip based direct triple antibody immunoassay for monitoring patient comparative response to leukemia treatment", Biomedical Microdevices, 22(3): 48, (2020).

[22] Uslu, F., Icoz, K., Tasdemir, K., Doğan, R. S. and Yilmaz, B., "Image-analysis based readout method for biochip: Automated quantification of immunomagnetic beads, micropads and patient leukemia cell", Micron, 133: 102863, (2020).

[23] Hejazian, M., Li, W. and Nguyen, N.-T., "Lab on a chip for continuous-flow magnetic cell separation", Lab Chip, 15(4): 959–970, (2015).

[24] Nguyen, N. T., "Micro-magnetofluidics: Interactions between magnetism and fluid flow on the microscale", Microfluidics and Nanofluidics, 12: 1-6, (2012).

[25] Ablay, G., Böyük, M. and İçöz, K., "Design, modeling, and control of a horizontal magnetic micromanipulator", Tranactions of Institute of Measurement and Control, 41(11): 3190-3198, (2019).

[26] Washburn, E. W., "The dynamics of capillary flow", Physical Review, 17(3): 273-283, (1921).

[27] Li, H. "Qualitative Blood Coagulation Test Using Paper-Based Microfluidic Lateral Flow Device", MSc. Thesis, University of Cincinnati, School of Electrical Engineering and Computing Science, (30-40), 2014.

[28] Gong, M. M. and Sinton, D., "Turning the Page: Advancing Paper-Based Microfluidics for Broad Diagnostic Application", Chemical Reviews, 117(12): 8447-8480, (2017).

[29] Cummins, B. M., Chinthapatla, R., Ligler, F. S. and Walker, G. M., "Time-Dependent Model for Fluid Flow in Porous Materials with Multiple Pore Sizes", Analytical Chemistry, 89(8): 4377–4381, (2017).

[30] Walji, N. and MacDonald, B. D., "Influence of Geometry and Surrounding Conditions on Fluid Flow in Paper-Based Devices", Micromachines, 7(5): 73, (2016).

[31] Chan, B.D., Mateen, F., Chang, C.L., Icoz, K. and Savran, C. A., "A compact manually actuated micromanipulator", Journal of Microelectromechanical Systems, 21(1): 7–9, (2012).

[32] Icoz, K., Soylu, M. C., Canikara, Z. and Unal, E., "Quartz-crystal Microbalance Measurements of CD19 Antibody Immobilization on Gold Surface and Capturing B Lymphoblast Cells: Effect of Surface Functionalization", Electroanalysis, 30(5): 834–841, (2018).